Earth Surface Processes and Landforms
Earth Surf. Process. Landforms **33**, 1157–1173 (2008)
Published online 21 November 2007 in Wiley InterScience
(www.interscience.wiley.com) **DOI:** 10.1002/esp.1603

The behavior of specific sediment yield in different grain size fractions in the tributaries of the middle Yellow River as influenced by eolian and fluvial processes

Jiongxin Xu*
Institute of Geographical Sciences and Natural Resources Research, Chinese Academy of Sciences; Key Laboratory of Water Cycle and Related Land Surface Processes, Chinese Academy of Sciences, Beijing, China

**Correspondence to: Jiongxin Xu, Institute of Geographical Sciences and Natural Resources Research, Chinese Academy of Sciences; Key Laboratory of Water Cycle and Related Land Surface Processes, Chinese Academy of Sciences, Beijing 100101, China. E-mail: xujx@igsnrr.ac.cn*

Received 18 October 2006;
Revised 28 June 2007;
Accepted 12 July 2007

Abstract

Based on data from 35 stations on the tributaries of the Yellow River, annual specific sediment yield (Y_s) in eight grain size fractions has been related to basin-averaged annual sand–dust storm days (D_{ss}) and annual precipitation (P_m) to reveal the influence of eolian and fluvial processes on specific sediment yield in different grain size fractions. The results show that Y_s in fine grain size fractions has the highest values in the areas dominated by the coupled wind–water process. From these areas to those dominated by the eolian process or to those dominated by the fluvial process, Y_s tends to decrease. For relatively coarse grain size fractions, Y_s has monotonic variation, i.e. with the increase in D_{ss} or the decrease in P_m, Y_s increases. This indicates that the sediment producing behavior for fine sediments is different from that for relatively coarse sediments. The results all show that Y_s for relatively coarse sediments depends on the eolian process more than on the fluvial process, and the coarser the sediment fractions the stronger the dependence of the Y_s on the eolian process. The Y_s–D_{ss} and Y_s–P_m curves for fine grain size fractions show some peaks and the fitted straight lines for Y_s–D_{ss} and Y_s–P_m relationships for relatively coarse grain size fractions show some breaks. Almost all these break points may be regarded as thresholds. These thresholds are all located in the areas dominated by the coupled wind–water process, indicating that these areas are sensitive for erosion and sediment production, to which more attention should be given for the purpose of erosion and sediment control. A number of regression equations were established, based which the effect of rainfall, sand–dust storms and surface material grain size on specific sediment yield can be assessed.

Keywords: erosion; specific sediment yield; sediment grain size; coupled wind–water process; Yellow River basin

Introduction

Fluvial sediment is non-uniform and consists of a number of grain size fractions, from relatively coarse to very fine ones. Much research has been performed on suspended sediment of rivers, especially the grain size aspect (ASCE Task Committee on Preparation of Sedimentation Manual, 1975; Walling and Moorehead, 1987, 1989; Walling and Webb, 1992; Grimshaw and Lewin, 1980; Peart and Walling, 1982; Reid and Frostick, 1994; Asselman, 1999). Although specific sediment yield is a topic drawing attention from many researchers, most of the research takes the specific sediment yield (Y_s) in all grain size fractions as a whole, and does not differentiate the Y_s in different grain size fractions.

Sediment carrying flows in rivers, especially hyperconcentrated flows in the Yellow River and its tributaries, can be regarded as a two-phase flow (Chien and Wan, 1998; Zhao, 1996). Its behavior depends on the solid phase and the liquid phase; the latter is a quasi-homogeneous mixture of water and fine sediment. The interaction between the solid and liquid phases results in some complicated behavior of hyperconcentated flows, especially their sediment transport

behaviors (Xu, 2002a). When the coupled wind–water process is considered, the behavior is more complicated. In our previous study (Xu *et al.*, 2006), we studied the influences of coupled wind–water process on suspended sediment grain size in the tributaries of the Yellow River. In the present study, we will further study the behavior of sediment production in different grain size fractions as influenced by eolian and fluvial processes, an issue that has not been dealt with so far.

The cause of strong sediment deposition in the lower Yellow River is a topic of significance both in theory and in engineering practice related to harnessing the Yellow River. The amount of sediment deposition depends not only on the amount of sediment supplied from the drainage basin, but also on its grain size composition. The study by Chien *et al.* (1980) indicated that the sediment contributing the most to the deposition of the lower Yellow River is that coarser than 0·05 mm, which comes mainly from the drainage area between Hekouzhen and Longmen and the Beiluohe and Malainhe River basins, known as the 'relatively coarse sediment producing area' in the middle Yellow River. The study by Xu and Cheng (2002) shows that, for each ton of sediment supplied from this 'relatively coarse sediment producing area', 0·455 ton was deposited in the lower Yellow River channel; however, for each ton of sediment supplied from the 'fine sediment producing area' between Longmen and Sanmenxia, only 0·155 ton was deposited in the lower Yellow River channel. Thus, the former is almost three times the latter. Therefore, the issue of sediment source and grain size composition in the Yellow River basin are of particular concern to researchers, with many results published. The distribution of the 'coarse sediment producing area' and its area has been identified (Chien *et al.*, 1980; Tang, 1990; Xu and Niu, 2000). The complicated relationship between fluvial sediment concentration and water discharge has been found (Xu, 2002b), and it has also been found that there exists an 'optimal' grain size composition, at which the suspended sediment concentration of hyperconcentrated flows attains the maximum (Xu, 1997). The relationship between specific sediment yield (Y_s) and drainage area (A) has been studied. With increasing basin area, the specific sediment yield increases, reaches a maximum and then declines. The non-linear variation in the Y_s–A relationship can be explained by surface material distribution, adjustment of the basin at macro time- and space scales and the variation of energy expenditure with drainage-basin scale (Xu and Yan, 2005).

The middle Yellow River, especially its tributaries such as the Kuyehe, Wudinghe and Tuweihe Rivers in this area, are located in the transitional zone from desert to loess. From this area, the sediment supply to the Yellow River is relatively coarse, and hyperconcentrated flows are well developed there. Thus, this area is ideal to study sediment yield by the coupled wind–water process.

Outline of Study Area, Data and Methodology

Outline of study area

More than 29 rivers are involved, which are located in the middle Yellow River, mainly in the area between Hekouzhen and Longmen. These include all tributaries of the Yellow River in which long term and systematical sampling and analysis of suspended sediment grain size have been done at hydrometric stations. The study area is located in a transitional zone from eolian sand to loess, and also a transitional zone from arid to semi-arid and sub-humid climates. From northwest to southeast, annual mean precipitation increases from 200 to 600 mm, annual mean number of days with strong wind (defined as a wind with maximum wind velocity higher than 17 m/s, a standard used in meteorological observations in China (Zhu, 1982)) decreases from 40 to 10 days and annual mean number of sand–dust storm days decreases from 25 to 5. Apart from some bedrock outcrops, the types of surface material are closely related to wind actions. From northwest to southeast, eolian sand, sandy loess, (typical) loess and clayey loess appear (Liu, 1964). Between the eolian sand and sandy loess areas, a transitional zone can be seen, where loess is covered by eolian sand patches. The so-called 'relatively coarse sediment producing area' (Chien *et al.*, 1980), the major sediment-contributing source area of the Yellow River, is located in the study area. According to the data from 1954 to 1995, the annual suspended sediment load coarser than 0·05 mm was $24\,519 \times 10^4$ tons, of which $12\,928 \times 10^4$ tons are from the Kuyehe, Wudinghe, Huangfuchuan and Gushanchuan Rivers (Xu and Niu, 2000), accounting for 52·7% of the total.

Data

In the study area, the coupled wind–water process is typical. Wind and water processes alternate seasonally. In winter and spring wind action is dominant, and entering summer, the rainy and high-flow season, fluvial action becomes dominant (Xu, 1998). Because annual precipitation increases and annual sand–dust storm days decrease from northwest to southeast, different spatial combinations of wind with water processes occur. In the northwest wind action is dominant in the coupled wind–water process, and in the southeast water action is dominant. From a macroscopic point of view,

DOI: 10.1002/esp

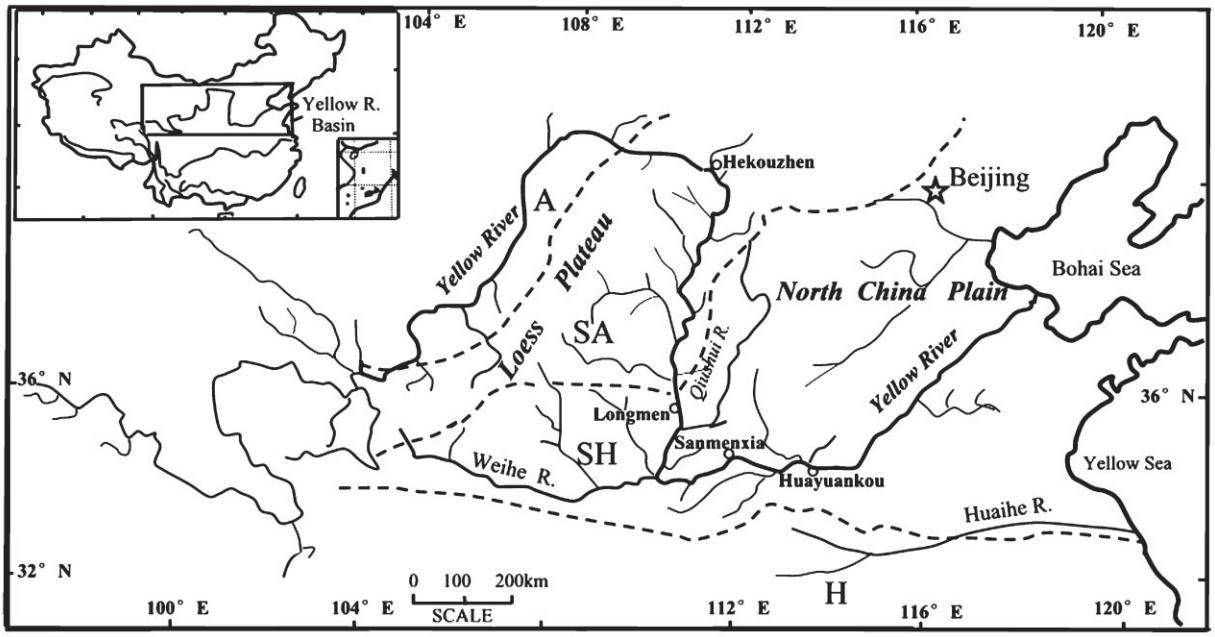

Figure 1. Location of study area. Dished lines are boundary between climates. H, humid; SH, sub-humid; SA, semi-arid; A, arid.

annual mean precipitation (P_m) is taken as an index for water processes, and annual mean number of sand–dust storm days (D_{ss}) and strong wind (D_{sw}) for wind processes. Transport by wind depends not only on the velocity of the wind, but also on the availability of dry sand or other loose, fine erodible material. If the latter is not available, the eolian sand transport is very low. Frequent occurrence of sand–dust storms means that both conditions mentioned above are met. Thus, D_{ss} is taken as an index that reflects both the intensity of the wind and the sand–dust transfer by the wind.

The Yellow River Commission has established a network of hydrometric stations and rain gauges in the Yellow River drainage basin, including the study area. A network of meteorological stations is also established by the local government. The data of precipitation and sand–dust storms are all from these rain gauges and meteorological stations for the period from 1950 to 1985. To get the annual mean precipitation for river drainage basins, area-weighted average was calculated, based on the data from the involved gauges. However, the annual mean number of sand–dust storm days for river drainage basins is the arithmetic mean, because in some river basins the number of meteorological stations is much fewer than that of rain gages.

In the suspended-sediment grain size analysis in the study area, ten fractions for grain size (D) are categorized: (1) less than 0·007, (2) 0·007–0·01, (3) 0·01–0·025, (4) 0·025–0·05, (5) 0·05–0·10, (6) 0·10–0·25, (7) 0·25–0·50, (8) 0·50–1·0, (9) 1·0–2·0 and (10) 2·0–5·0 mm. Because the last two fractions appear only in a very few hydrometric stations, Classes (1)–(8) are adopted in the present study. The specific sediment yield (Y_s) is calculated as $Y_s = Q_s/A$, where Q_s is annual suspended sediment load at the station and A is the drainage area above the station. If the weight percentage of the a given grain size fraction of the total annual sediment load is P_i, then the specific sediment yield in this fraction is $Y_{s,i} = Y_s P_i$. Here P_i is for any one of the classes (1)–(8) above.

The data of annual suspended load and grain size composition used in this study are collected at 35 hydrometric stations on rivers involved. The period from which the data were used is from 1950 to 1970 as basin-wide erosion and sediment control measures have not yet been practiced during this period, and human impact on sediment producing and transporting processes was relatively small. The hydrometric stations selected in this study are those where both sediment load and grain size are measured.

Method

After calculating the specific sediment yield for the above eight fractions, relationships are established between them and annual precipitation and annual number of sand–dust storm days, to reveal how the specific sediment yield in different grain size varies with fluvial and eolian actions, and identify some thresholds. Then, multiple regression analysis is performed to establish the relationship between specific sediment yield and the influencing factors.

DOI: 10.1002/esp

Results

Specific sediment yield in different grain size fractions varying with wind action

Based on data from the studied rivers, mean annual specific sediment yield (Y_s) for five fine grain size fractions has been plotted against basin-averaged mean annual number (D_{ss}) of sand–dust storms in Figure 2. The five fine grain size fractions include those with grain size (1) less than 0·007, (2) 0·007–0·01, (3) 0·01–0·025, (4) 0·025–0·05 and (5) 0·05–0·10 mm. It can be seen from Figure 2 that for all five fractions the Y_s–D_{ss} curves show some common trends. With increase in D_{ss}, Y_s increases to a peak at $D_{ss} = 6$, followed by a decline. Thus, $D_{ss} = 6$ days is a threshold at which an abrupt turn occurs in the Y_s–D_{ss} relationship. Xu (2005a) found that there is a strong negative correlation between mean annual sand–dust storm days and precipitation in the study area (Figure 3). Thus, a relatively low D_{ss} in a river basin means a high P_m there. In such a river basin, the fluvial process is dominant. On the other hand, in a river basin

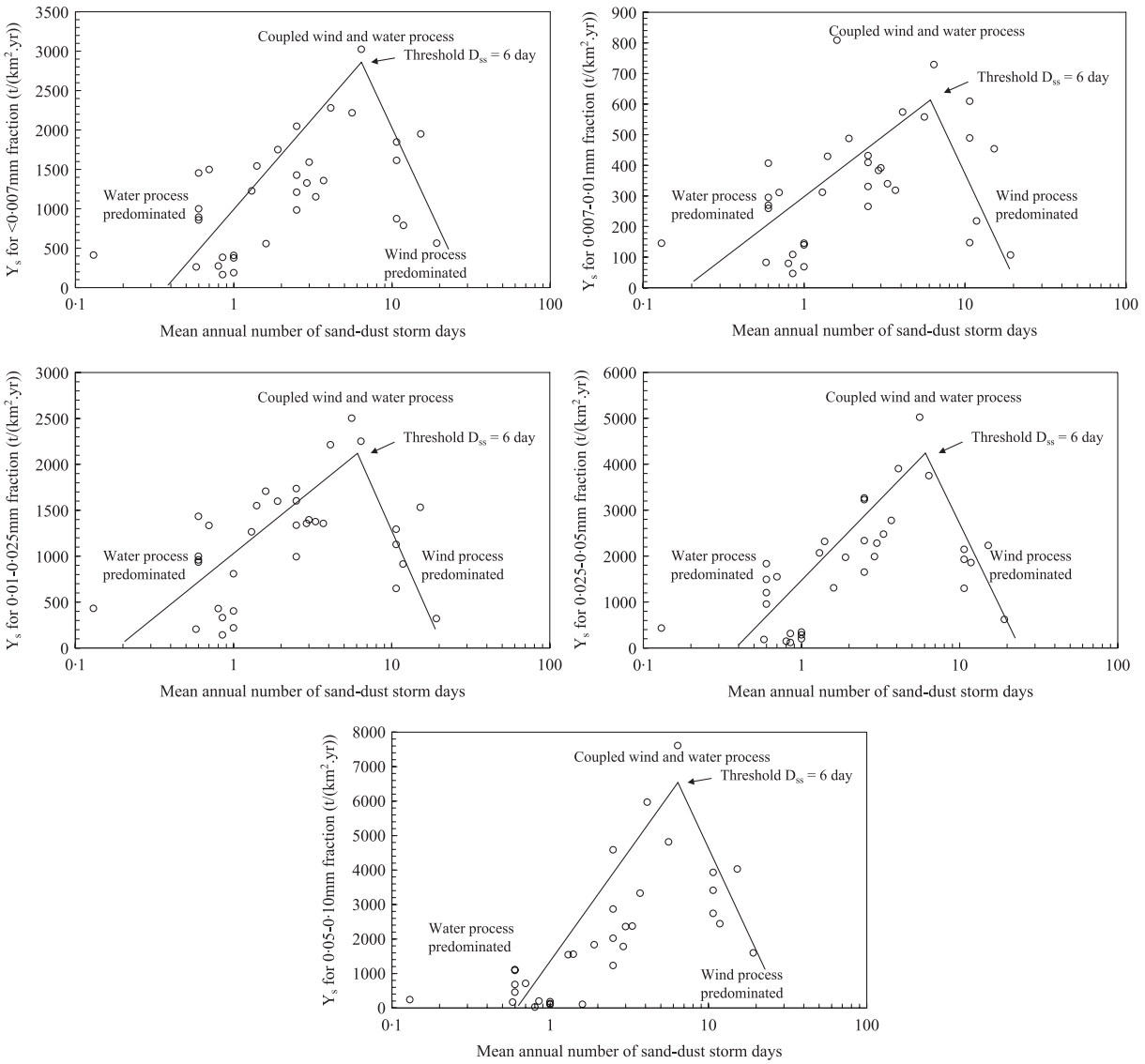

Figure 2. Relationships between specific sediment yield and mean annual sand–dust storm days for five fine grain size fractions with grain size (1) less than 0·007, (2) 0·007–0·01, (3) 0·01–0·025, (4) 0·025–0·05 and (5) 0·05–0·10 mm. The curves are fitted by eye.

DOI: 10.1002/esp

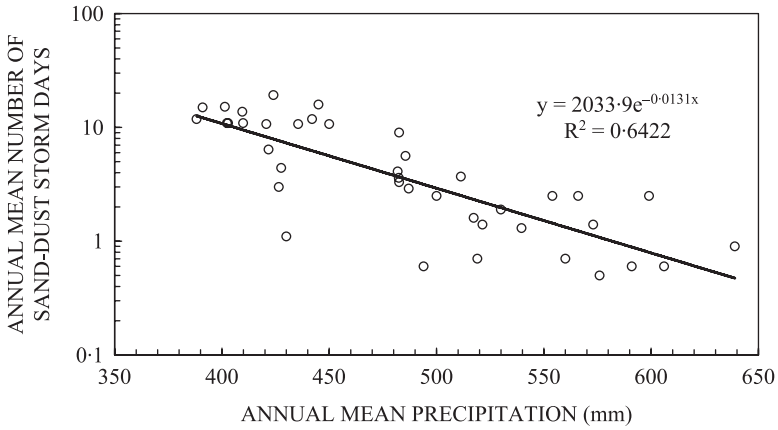

Figure 3. Relationship between mean annual precipitation and sand–dust storm days.

with a high D_{ss}, the P_m is low, and the wind process is dominant. In river basins with medium D_{ss}, both wind and fluvial processes are relatively strong, and the coupled wind–water process is dominant. Therefore, the five curves in Figure 2 imply that the specific sediment yield for fine grain size fractions is the highest in the river basins where the coupled wind–water process is dominant, and when going to the fluvial-process-dominant river basins or to the wind-process-dominant river basins the fraction specific sediment yield decreases.

Mean annual specific sediment yield for three relatively coarse grain size fractions has been plotted against basin-averaged mean annual number of sand–dust storms in Figure 4, with grain size (6) 0·10–0·25, (7) 0·25–0·50 and

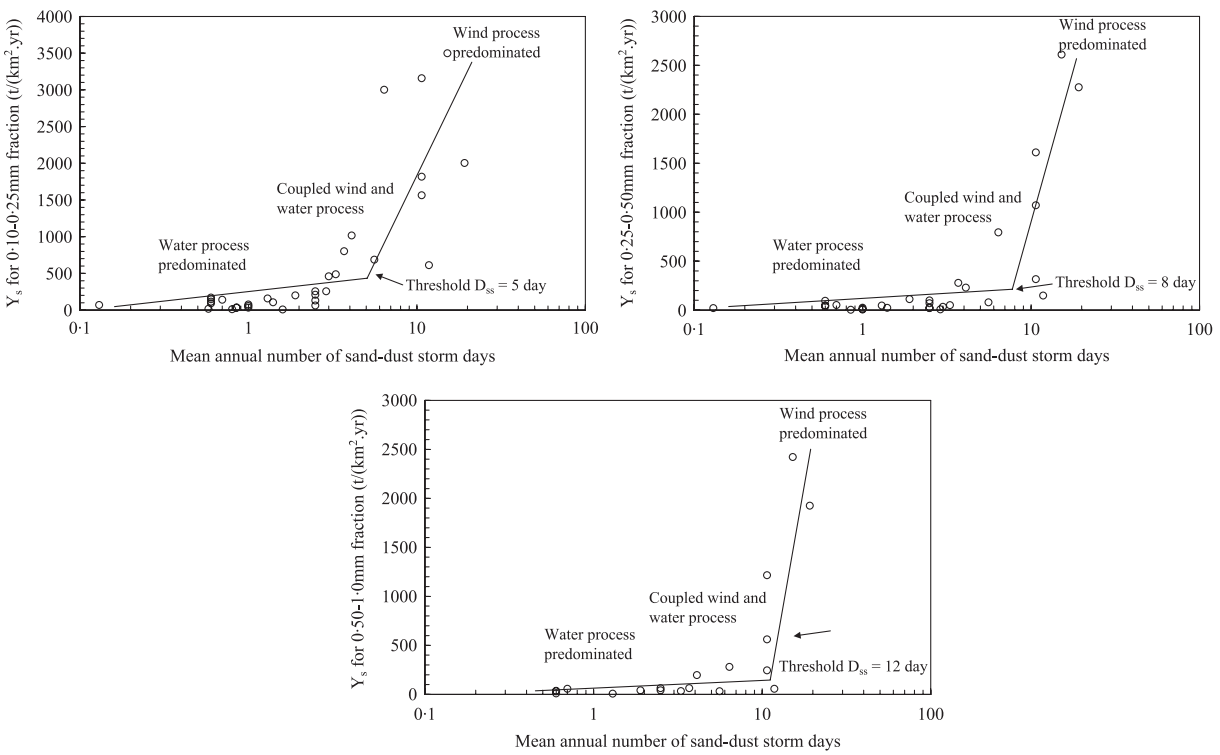

Figure 4. Relationships between specific sediment yield and mean annual sand–dust storm days for three relatively coarse grain size fractions. The curves are fitted by eye.

DOI: 10.1002/esp

(8) 0·50–1·0 mm. It can be seen that for the three coarse fractions the Y_s–D_{ss} curve shows monotonic variation, namely, Y_s increases with D_{ss}, a feature quite different from the curves for the five fine grain size fractions. This indicates that the sediment production behavior of coarse sediment fractions is different from that of the fine fractions. It is worth noting that, in the overall trend of increase, there is a break dividing all points into two groups that can be fitted by straight lines with different slopes. The slope of the line on the left-hand side is much gentler than the slope of the line on the right. This means that when the D_{ss} exceeds some threshold the rate at which Y_s increases with D_{ss} increases sharply. The D_{ss} at this threshold corresponding to the grain size fractions of 0·10–0·25, 0·25–0·50 and 0·50–1·0 mm is 5 days, 8 days and 12 days, respectively, indicating that the threshold increases with the grain size of the fractions. For the fraction of 0·10–0·25 mm, when D_{ss} is longer than 5 days, the fraction specific sediment yield starts to increase sharply. For the fraction of 0·25–0·50 mm, when D_{ss} exceeds 8 days, the fraction specific sediment yield starts to increase sharply. For the fraction of 0·50–1·0 mm, when D_{ss} exceeds 8 days, the fraction specific sediment yield starts to increase sharply. This indicates that the specific yield of coarse sediment strongly depends on wind process, and the coarser the sediment fraction is the more strongly the fraction specific sediment yield depends on wind process. It can also be seen that when going from the area dominated by the fluvial process to the area dominated by the coupled wind–water process, Y_s for coarse sediment fractions increases slowly. However, after entering the area dominated by the coupled wind–water process and going to the area dominated by the wind process, Y_s for coarse sediment fractions increases sharply.

Specific sediment yield in different grain size fractions varying with water action

Based on data from the studied rivers, mean annual specific sediment yield for four fine grain size fractions has been plotted against basin-averaged mean annual precipitation (P_m) of sand–dust storms in Figure 5. The four fine grain size fractions include those with grain size (1) less than 0·007, (2) 0·007–0·01, (3) 0·01–0·025 and (4) 0·025–0·05 mm. It can be seen from Figure 5 that for all four fractions the Y_s–D_{ss} curves show some common trends. With the increase in P_m, Y_s increases to a peak and then decreases. The P_m corresponding to the peak is 450 mm for the first two curves, and is 480 mm for the last two curves. Thus, $P_m = 450$ mm or $P_m = 480$ mm is regarded as a threshold at which an

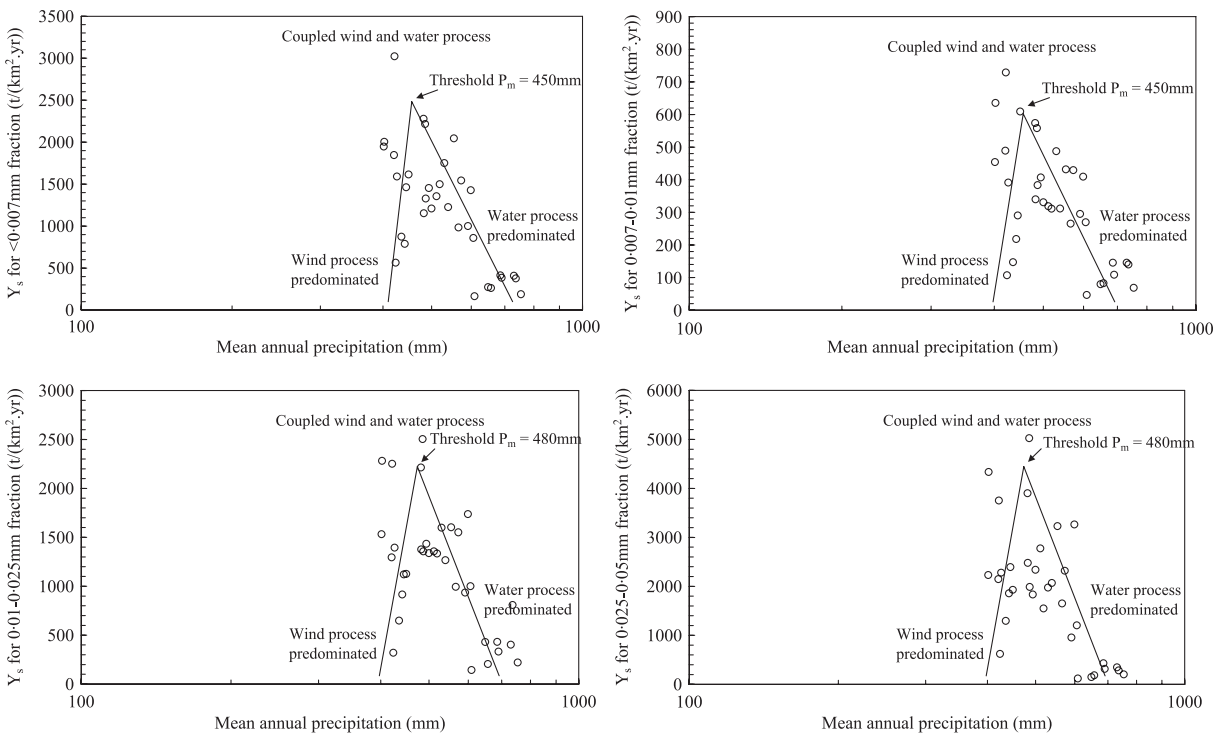

Figure 5. Relationships between specific sediment yield and mean annual precipitation for four fine grain size fractions. The curves are fitted by eye.

DOI: 10.1002/esp

abrupt turn occurs in the Y_s–P_m relationship. As shown in Figure 3, a relatively high P_m in a river basin means a low D_{ss} there. In such a river basin, the fluvial process is dominant. On the other hand, in a river basin with a low P_m, the D_{ss} is high, and the wind process is dominant. In river basins with a medium P_m, both wind and fluvial processes are relatively strong, and the coupled wind–water process is dominant. Therefore, the four curves in Figure 5 imply that the specific sediment yield for fine grain size fractions is the highest in the river basins where the coupled wind–water process is dominant, and when going to the fluvial-process-dominant river basins or to the wind-process-dominant river basins the fraction specific sediment yield decreases.

Mean annual specific sediment yield for four relatively coarse grain size fractions has been plotted against basin-averaged mean annual number of sand–dust storms in Figure 6, with grain size (1) 0·05–0·10, (2) 0·10–0·25, (3) 0·25–0·50 and (4) 0·50–1·0 mm. It can be seen that for the four coarse fractions the Y_s–P_m curve shows monotonic variation, namely, Y_s decreases with P_m, a feature quite different from the curves for four fine grain size fractions. This indicates that the sediment production behavior of coarse sediment fractions is different from that of the fine fractions. It is worth noting that, in the overall trend of decrease, there is a break dividing all points into two groups that can be fitted by straight lines with different slopes. The slope of the line on the left-hand side is much steeper than the slope of the line on the right. This means that when P_m exceeds some threshold, the rate at which Y_s increases with P_m decreases sharply. The thresholds of P_m corresponding to the 0·05–0·10, 0·10–0·25, 0·25–0·50 and 0·50–1·0 mm grain size fractions are 530, 500, 470 and 450 mm, respectively, indicating a trend of decrease with grain size. For the fraction of 0·05–0·10 mm, when P_m is larger than 530 mm, the fraction specific sediment yield starts to decrease sharply. For the fraction of 0·10–0·25 mm, when P_m is larger than 500 mm, the fraction specific sediment yield starts to decrease sharply. For the fraction of 0·25–0·50 mm, when P_m is larger than 470 mm, the fraction specific sediment yield starts to decrease sharply. For the fraction of 0·50–1·0 mm, when P_m is larger than 450 mm, the fraction specific sediment yield starts to decrease sharply. Similarly to the foregoing discussion related to D_{ss}, this indicates that the specific sediment yield of coarse sediment strongly depends on the wind process. When going from the area dominated by the fluvial process to the area dominated by the coupled wind–water process, Y_s for coarse sediment fractions increases slowly. However, after entering the area dominated by the coupled wind–water process and going to the area dominated by the wind process, Y_s for coarse sediment fractions increases sharply.

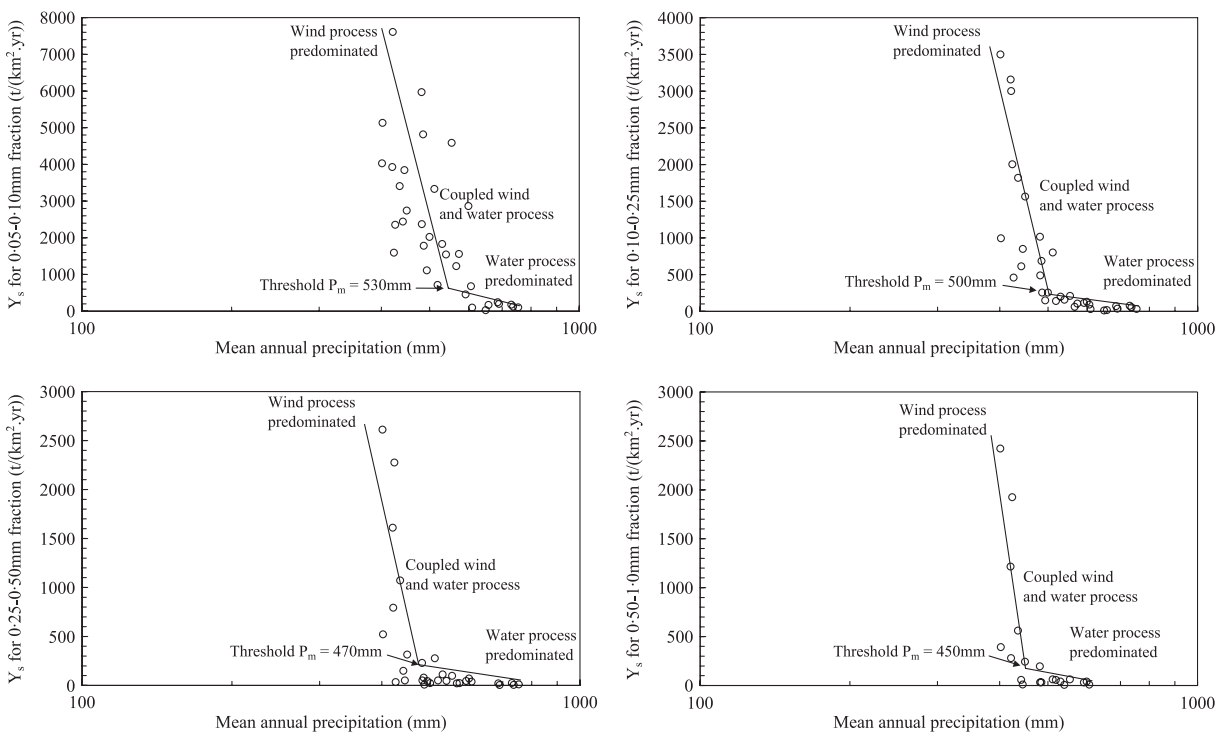

Figure 6. Relationships between specific sediment yield and mean annual precipitation for four relatively coarse grain size fractions. (1) 0·05–0·10, (2) 0·10–0·25, (3) 0·25–0·50 and (4) 0·50–1·0 mm. The curves are fitted by eye.

DOI: 10.1002/esp

Explanation

Langbein and Schumm (1958) established the relationship between specific sediment yield and effect annual precipitation, using data from rivers in the United States. They found that specific sediment yield increases with effect annual precipitation to a peak, followed by a decline. This curve has therefore been called the Langbein–Schumm curve, and applied to many rivers in other countries. In fact, the curves in Figure 5 may be regarded as the Langbein–Schumm curves for rivers on the Loess Plateau. Because a close positive correlation exists between annual precipitation and sand–dust storm days (Figure 3), the curves in Figure 2 may also be regarded as extensions of Langbein–Schumm curves. It is worth noting that for fine sediment fractions the Y_s–P_m relationship can be described by the Langbein–Schumm curve because Y_s increases with P_m to a peak and then decreases. However, from relatively coarse sediment fractions, the Y_s–P_m relationship cannot be described by the Langbein–Schumm curve because Y_s increases with P_m monotonically and no peak appears. This indicates again that the sediment production behavior of coarse grain size fractions is different from that of fine fractions, following different regularities. The cause for this is discussed as follows.

Let us first consider relatively fine sediment (grain size (D) less than 0·1 mm, see Figures 2 and 5). In areas dominated by the wind process (with high D_{ss}, see the right-hand side of the curves in Figure 2, or, with low P_m, see the left-hand side of the curves in Figure 5), the dominant vegetation type is desert shrub or dry steppe with low cover percentages. The protection of vegetation against erosion is weak. However, on the other hand, precipitation is low, and the land surface material is eolian sand or loess covered by patched eolian sand, which is highly permeable. Thus, surface runoff is weak, and erosion by water is also weak. On the other hand, in areas dominated by the fluvial process (with low D_{ss}, see the left-hand side of the curves in Figure 2; or, with high P_m, see the right-hand side of the curves in Figure 5), rainfall is abundant and therefore rainfall erosivity is high. However, the abundant rain favors growth of forest, which effectively protects the land surface against erosion. Moreover, on the Loess Plateau, with the increase in P_m from northwest to southeast, the grain size of the loess becomes finer and finer (Liu, 1964). Thus, in areas with a high P_m, the surface material is clayey loess, the erosion resistance of which is relatively high. Therefore, erosion intensity and specific sediment yield are also low. In the areas between the above two extremes, both D_{ss} and P_m are moderately high, and erosion and sediment yield are dominated by the coupled wind–water process. Although annual precipitation is low, it is often concentrated as one or two rainstorms with high rainfall intensity. The dominant vegetation is steppe, whose resistance to wind erosion or water erosions is both weak. The surface material is sandy loess, which is highly erodible. Thus, the erosion intensity is high. It is more important that in these areas there is a particular mechanism of erosion induced by seasonally alterative wind and water processes, as described by Xu *et al.* (2006). In winter and spring, strong wind transports eolian sand and other coarse material derived from weathered bedrock into gullies, river channels and floodplains, where they are stored temporarily. In the following summer, raindrops and storm runoff erode loess on slopeland, and the resulting turbid water rushes into gullies and river channels. Previously stored coarse material is rapidly set in suspension and hyperconcentrated flows form. By this process, most of the previously stored eolian sands and the material supplied by mass-wasting of loess can be transported downstream, leading to very high specific sediment yield. Thus, a high value of Y_s occurs in these areas.

For relatively coarse sediment with $D > 0{\cdot}1$ mm (see Figure 4), specific sediment yield increases with D_{ss} monotonically, but there exists a threshold. When crossing it, the rate at which Y_s increases with D_{ss} increases sharply. This is because in areas with a weak wind process the surface material is clayey loess, the supply of coarse sediment is very limited and thus the specific sediment yield for coarse grain size fractions is low. With the increase in D_{ss}, the wind process becomes stronger, the surface material becomes sandy loess or sandy loess covered by eolian sand patches and thus the supply of coarse sediment increases. Due to the mechanism of erosion induced by seasonally alternating wind and water processes mentioned above, the coarse sediment carried to gullies and river channels by wind during winter and spring can be further transported downstream along the river, by turbid rainstorm runoff from loess hillslopes. As a result, Y_s for coarse sediment fractions can reach a very high magnitude. The thresholds in Figure 4, from which Y_s increases abruptly, implies that, on entering the area dominated by the coupled wind–water process, erosion, sediment transport and sediment yield are all greatly intensified. Moreover, Figure 4 shows that the thresholds of D_{ss} corresponding to the grain size fractions of 0·10–0·25, 0·25–0·50 and 0·50–1·0 mm are 5, 8 and 12 days, respectively, indicating that the thresholds increases with grain size. This is because the grain size of sand that is carried by the wind is positively correlated with wind velocity (Chien and Wan, 1983), namely, the coarser the sand, the higher the wind velocity needed to carry the sand. Based on data from 200 stations in the Yellow River basin, the correlation between D_{ss} and mean annual wind velocity was established, indicating a significance level of less than 0·01 (Xu, 2005b). Only when the wind velocity or D_{ss} reaches sufficiently high values can the coarse sediment be effectively eroded and transported. Thus, the thresholds of D_{ss} increase with grain size of the sediment fractions.

For the relatively coarse sediment with $D > 0{\cdot}05$ mm (see Figure 6), Y_s decreases with P_m monotonically, but there exists a threshold. When P_m is lower than the P_m at this threshold, Y_s decreases abruptly. The formative mechanism for

DOI: 10.1002/esp

Table I. Correlation coefficients of D_{ss} and P_m with Y_s in eight grain size fractions

	Specific sediment yield (t/(km^2 yr)) for each grain size (mm)							
	<0·007	**0·007–0·01**	**0·01–0·025**	**0·025–0·05**	**0·05–0·10**	**0·10–0·25**	**0·25–0·50**	**0·50–1·0**
P_m	−0·278 36	−0·223 99	−0·070 3	−0·167 58	−0·520 74	−0·723 79	−0·585 05	−0·544
D_{ss}	−0·040 65	−0·089 82	−0·251 75	−0·056 04	0·351 863	0·700 464	0·729 39	0·811 2

this is similar to that for the variation in Figure 3. In areas with relatively low P_m, the wind process is strong, the surface material is eolian sand and sandy loess and thus the coarse sediment supply is abundant. There may exist a coupled wind–water process, which results in high specific sediment yield for coarse grain size fractions. With the increase in P_m, the wind process becomes weaker, the surface material becomes typical loess and clayey loess and the coarse sediment supply is very limited. Hence, Y_s for coarse sediment fractions decreases sharply.

Figures 2 and 4–6 all indicate a non-linear relationship of Y_s with D_{ss} and P_m. Among them, the relationships in Figures 2 and 5 are complicated; i.e., Y_s increases first, reaches a peak and then decreases. The variation in Figures 4 and 6 is monotonic, but a break appears. Strictly speaking, for complicated variations, calculation of a simple correlation coefficient for comparison is not reasonable. However, as a first approximation, the correlation coefficients of Y_s with D_{ss} and P_m for different grain size fractions have been calculated (Table I), and then the correlation coefficient plotted against the class of grain size fractions (Figure 7). It can be seen that for fine sediment fractions less than 0·05 mm, the Y_s–D_{ss} correlation coefficient is rather low. When grain size exceeds 0·05 mm, the correlation coefficient becomes positive and increases rapidly. All the Y_s–P_m correlation coefficients are negative, and the Y_s–P_m correlation coefficient is negatively correlated with grain size, namely, the Y_s–P_m correlation coefficient increases with grain size. In other words, as the grain size becomes coarser, the Y_s is correlated with P_m more closely. The fact that the Y_s–D_{ss} and Y_s–P_m correlations become closer with the increase in grain size indicates that the response of fine sediment fractions to the spatial variation in precipitation and sand–dust storms is not sensitive, but the response of coarse fractions is more sensitive, and the sensitivity increases with sediment grain size. Therefore, when the source of relatively coarse sediment of the Yellow River basin is studied, sufficient attention should be paid to the spatial variation in fluvial and eolian processes, and then the areas delineated where the natural conditions most favor erosion and sediment yield of relatively coarse sediment. On this basis, investment could be concentrated on these areas, for the purpose of controlling the relatively coarse sediment, which is most harmful to the lower Yellow River channel.

In this study a number of thresholds have been determined. Although P_m or D_{ss} at these points varies, they are all located in the zone dominated by the coupled wind–water process. This indicates again that this zone is a sensitive zone for erosion and sediment yield, to which more attention should be given.

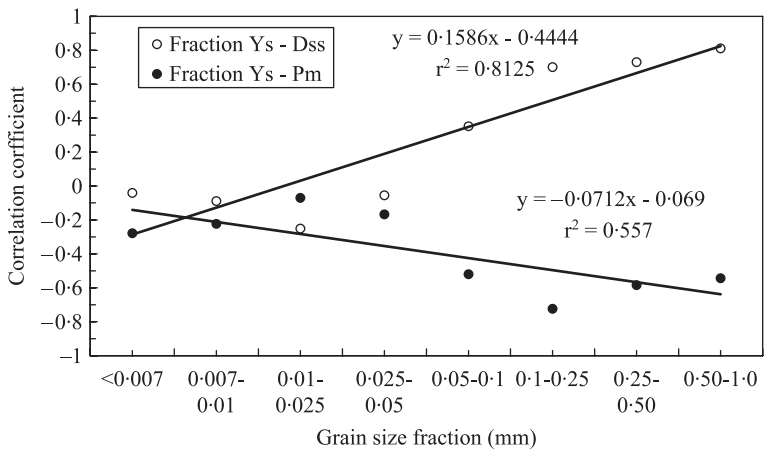

Figure 7. Correlation coefficients of D_{ss} and P_m with Y_s in eight grain size fractions varying with grain size classes.

DOI: 10.1002/esp

Specific sediment yield as influenced by the spatial variation of influencing physico-geographical factors

To show how specific sediment yield is affected by physico-geographical factors, comparison has been made between their spatial distributions. Spatial variation of environmental characteristics such as mean annual precipitation, mean annual number of sand–dust storm days, types and grain size of loess, and vegetation types are shown in Figure 8(a)–(c), and the distribution of specific sediment yield is shown in Figure 8(d), based on data from the Yellow River basin. The Loess Plateau is characterized by a northwest-to-southeast decrease in number of sand–dust storms and an increase in rainfall. Along the same direction, the grain size of the loess becomes finer, meaning an increase in clay percentage in the loess and therefore a decline in soil erodibility. The spatial variation in vegetation types is strongly controlled by precipitation, and the boundary lines of vegetation types are approximately parallel to the rainfall iso-lines. Due to the latter two, the erodibility of the land surface decreases from northwest to southeast. As eolian deposits, the deposition of loess occurred at geological timescales (Liu, 1964). However, the grain size of loess on the land surface can still be related to mean annual precipitation and sand-storm days observed at present (Figure 9), and close correlation can be clearly seen. This means that climate affects not only vegetation, but also the grain size property of the loess, and through the latter the erosion process can be further affected.

Controlled by the spatially varying environmental factors, specific sediment yield exhibits a clear decreasing trend from northwest to southeast. It can be seen clearly that there is a high-value zone of specific sediment yield, stretching from northeast to southwest, and some high-value centers of Y_s appear in this zone (Figure 8(d)). Comparing Figure 8(d) with the map of distribution of annual precipitation and annual sand storm days (Figure 8(a)), the map of distribution of surface materials (Figure 8(b)) and the map of distribution of vegetation types (Figure 8(c)), the following points can be observed.

First, the high-value zone of Y_s is parallel with the iso-lines of annual precipitation and annual number of sand–dust storm days. It is roughly located between the 400 and 500 mm precipitation iso-lines, and between the 10 and 15 day iso-lines of sand–dust storms. It can be thought that the high-value centers or 'peak-line' of Y_s are located roughly along the 450 mm precipitation iso-line, similar to the peak values of 450 or 480 mm which are observed from Figure 5.

Second, in the high-value zone of Y_s, Y_s deceases from northeast to southwest. At the northeast end it is more than 40 000 t/(km^2 yr), but at the southeast end it decreases to 10 000 t/(km^2 yr). The northeast end of the high-Y_s zone is located in the sandy loess zone, but the southwest end in the clayey loess zone. As an overall spatial variation, the loess becomes finer from northwest to southeast, and in the same direction Y_s decreases. The decreasing erodibility from the sandy loess zone to the clayey loess zone is also responsible for the spatial variation in specific sediment yield.

Third, the iso-lines of Y_s are roughly parallel with the boundary lines of vegetation types, and the high-value zone of Y_s is located in the steppe zone, similar to what is shown by the Langbein–Schumm relationship (Langbein and Schumm, 1958). Going to northwest from this high-value zone of Y_s one enters the semi-desert zone; and going to southeast from this high-value zone of Y_s one enters the deciduous broad-leaf forest. In both cases, the Y_s decreases, as shown by the iso-lines of Y_s in Figure 8(d) and the Y_s–rainfall plots in Figure 5.

To show the spatial variation further, the relationship between specific sediment yield and latitude has been plotted in Figure 10, based on data from the rivers studied. A decrease from north to south can be clearly seen. To study the spatial variation of specific sediment yields in eight grain size fractions, they were plotted against latitude, and regression equations were established. We also plotted the percentages of eight grain size fractions in suspended sediment against latitude, and established the regression equations. To save space, these graphs are not shown, but all the regression equations are given in Table II. The slope of the equations reflects the rate at which the variable changes with latitude. The specific sediment yield in all grain size fractions shows an increase from south to north, but the rate at which $Y_{s,f}$ increases with latitude is different. For three medium grain size fractions, i.e. 0·025–0·05, 0·05–0·10 and 0·10–0·25 mm, the rate is high, and for three relatively fine fractions (<0·007, 0·007–0·01 and 0·01–0·025 mm), or for two relatively coarse fractions (0·025–0·05 mm, 0·05–1·0 mm), the rate is low. It is notable that the latitudinal variations of percentage of eight grain size fractions in suspended sediment are complicated. For three relatively fine fractions (<0·007, 0·007–0·01and 0·01–0·025 mm) this percentage decreases from south to north, but for grain size fractions coarser than 0·025 mm this percentage increases from south to north. To see this more clearly, the regression lines for the latitudinal variation of percentage of eight grain size fractions in suspended sediment are given in Figure 11, where the original points are omitted.

Multiple statistical analysis

To determine the relationship between specific sediment yield and the influencing factors such as mean annual precipitation (P_m), mean annual number of sand–dust storm days (D_{ss}) and the grain size of surface material, multiple

DOI: 10.1002/esp

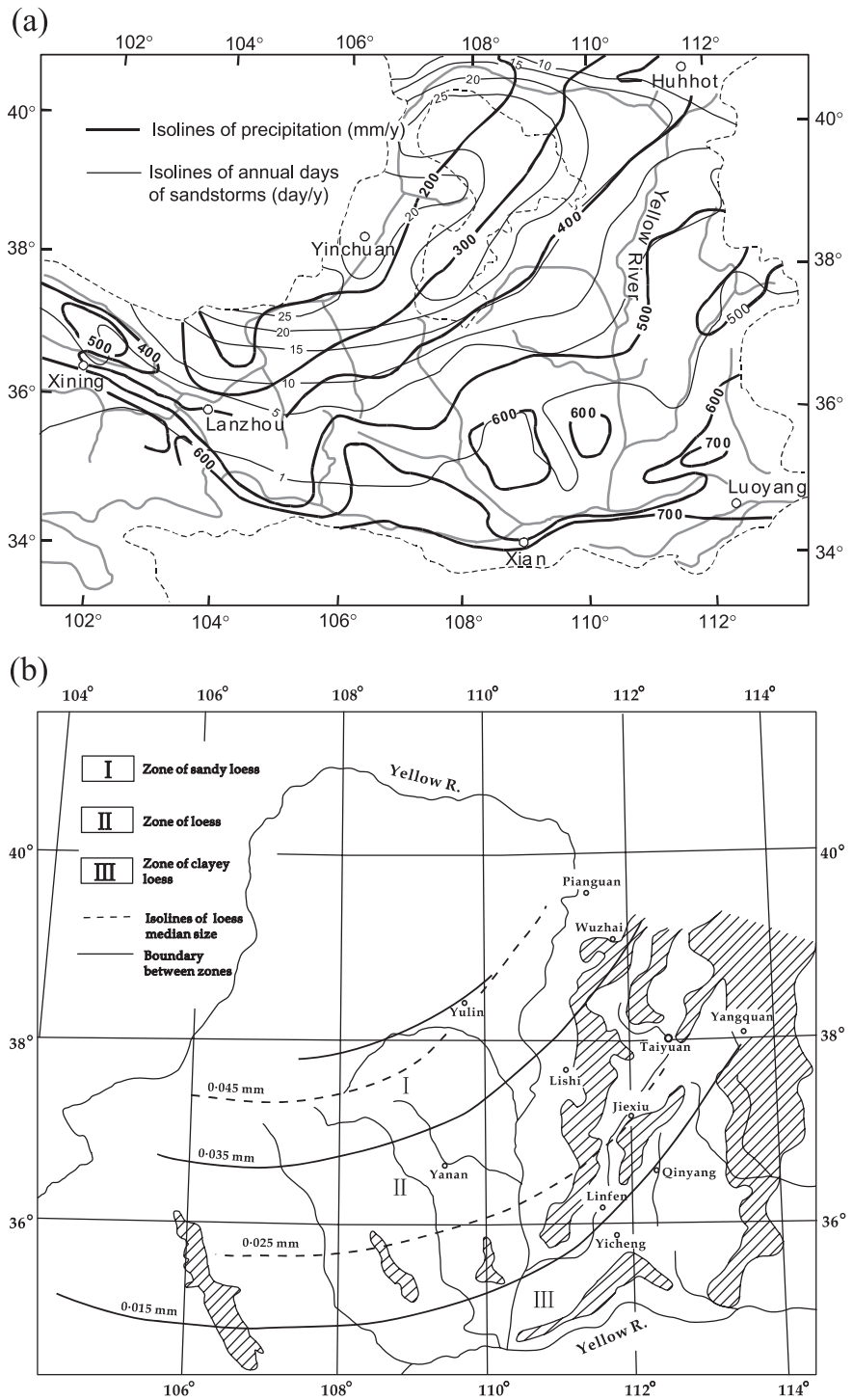

Figure 8. Spatial variation of environmental characteristics and specific sediment yield in the study area. (a) Distribution of annual precipitation and annual sand storm days. (b) Distribution of surface materials. (c) Distribution of vegetation types. I, deciduous broad-leaf forest; Ia, typical deciduous broad-leaf forest; Ib, deciduous broad-leaf forest with some sub-tropic component. II, steppe: IIa, steppe with forest; IIb, steppe zone. III, desert: IIIa, semi-desert; IIIb, desert. IV, meadow: IVa, high mountain meadow-steppe; IVb, cold meadow. V, evergreen broad-leaf forest. (d) Distribution of specific sediment yield. The map is re-drawn from the Compilation Commission of Bulletin of River Sedimentation in China (2003).

DOI: 10.1002/esp

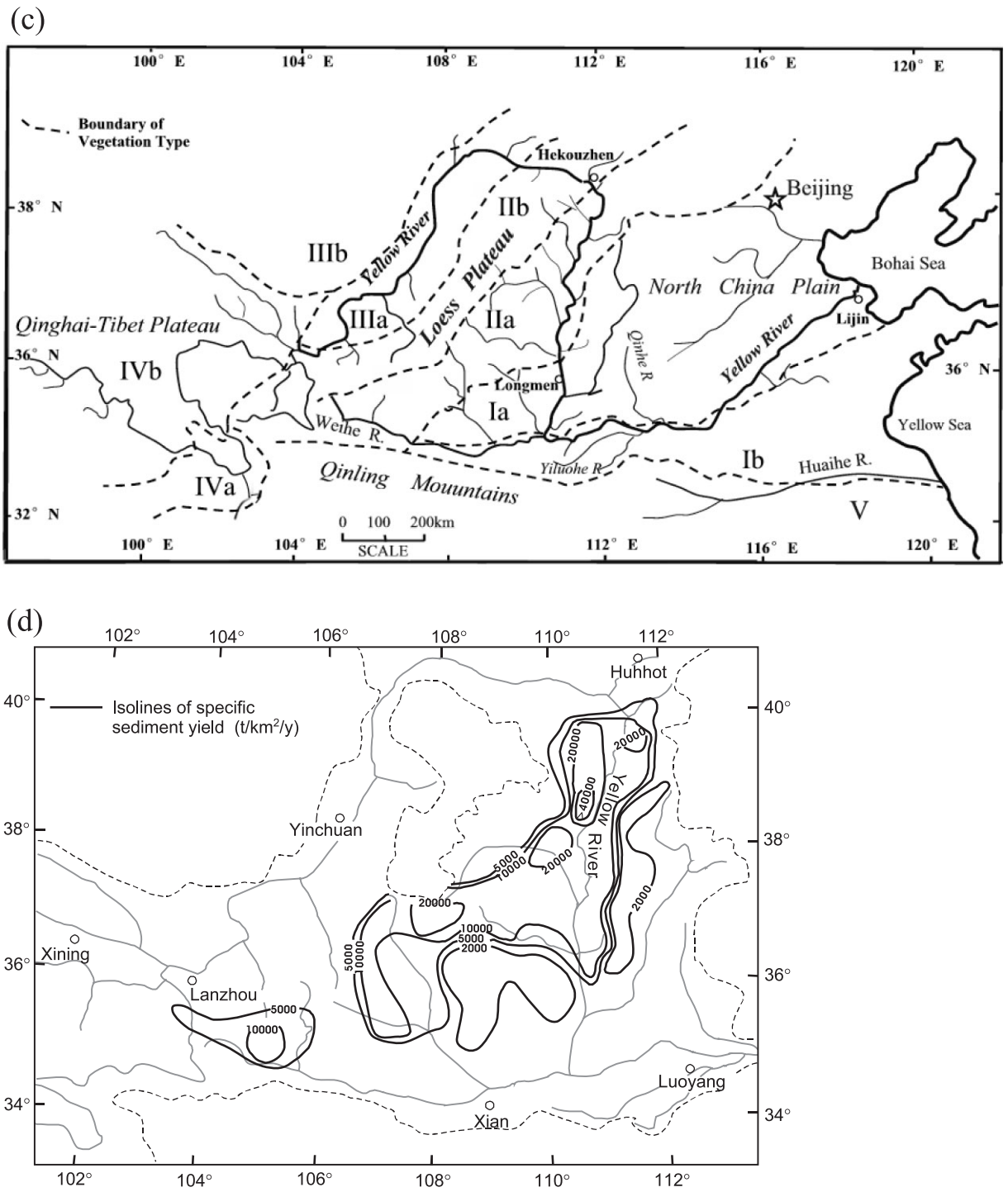

Figure 8. (*Continued*)

regression analysis was performed. Due to the lack of data for grain size of surface material, grain size characteristics of suspended sediment are used to reflect the former. On the Loess Plateau, loess is the major surface material type, and a close correlation was found between the median grain size in suspended sediment and the percentage of fractions larger than 0·05 mm in the loess (Figure 12). The correlation matrix between Y_s and influencing variables

DOI: 10.1002/esp

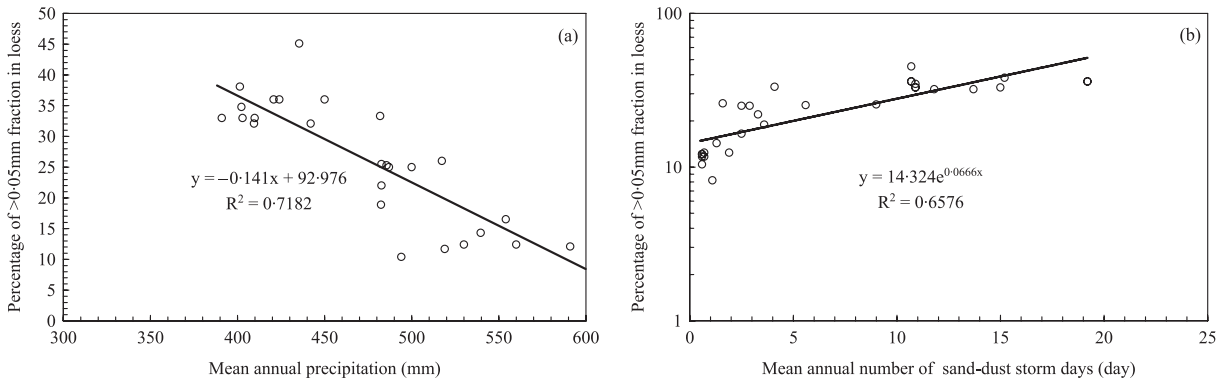

Figure 9. The percentage of grain size over 0·05 mm in loess as influenced by mean annual precipitation (a) and sand–dust storm days (b), based on data from the rivers studied.

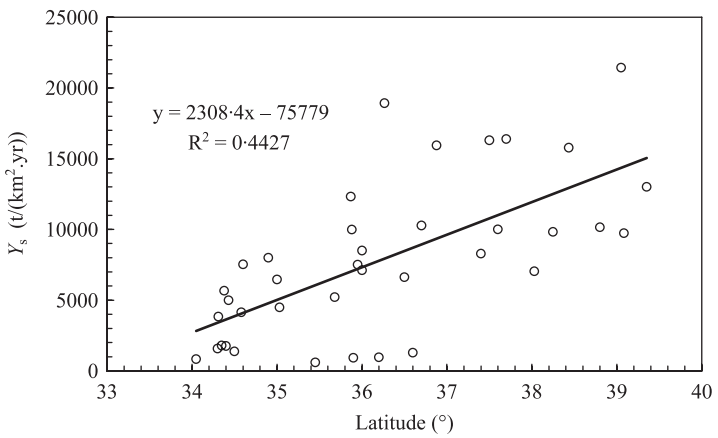

Figure 10. Specific sediment yield varying with latitude.

Table II. Regressions showing latitudinal variation in percentage (R_f) of eight grain size fractions in suspended sediment and that in fractional specific sediment yield ($Y_{s,f}$, in t/(km^2 yr)). Φ denotes latitude (°N)

Grain size fractions (mm)	Regression equation for latitudinal variation in percentage of given fraction	Regression equation for latitudinal variation in percentage of given fractional Y_s
<0·007	$R_f = -2{\cdot}4948\Phi + 108{\cdot}65$	$Y_{s,f} = 221{\cdot}79\Phi - 6828{\cdot}8$
	$r^2 = 0{\cdot}4459$, $p < 0{\cdot}01$	$r^2 = 0{\cdot}2395$, $p < 0{\cdot}01$
0·007–0·01	$R_f = -1{\cdot}0863\Phi + 44{\cdot}891$	$Y_{s,f} = 44{\cdot}502\Phi - 1275{\cdot}8$
	$r^2 = 0{\cdot}338$, $p < 0{\cdot}01$	$r^2 = 0{\cdot}1267$, $p < 0{\cdot}05$
0·01–0·025	$R_f = -1{\cdot}8537\Phi + 91{\cdot}004$	$Y_{s,f} = 123{\cdot}22\Phi - 3298{\cdot}8$
	$r^2 = 0{\cdot}2034$, $p < 0{\cdot}01$	$r^2 = 0{\cdot}096$, $p < 0{\cdot}10$
0·025–0·05	$R_f = 3{\cdot}6328\Phi - 109{\cdot}2$	$Y_{s,f} = 329{\cdot}12\Phi - 10\,116$
	$r^2 = 0{\cdot}368$, $p < 0{\cdot}01$	$r^2 = 0{\cdot}177$, $p < 0{\cdot}05$
0·05–0·1	$R_f = 2{\cdot}8346\Phi - 96{\cdot}351$	$Y_{s,f} = 804{\cdot}36\Phi - 27\,031$
	$r^2 = 0{\cdot}5809$, $p < 0{\cdot}01$	$r^2 = 0{\cdot}4542$, $p < 0{\cdot}01$
0·1–0·25	$R_f = 1{\cdot}5515\Phi - 53{\cdot}483$	$Y_{s,f} = 432{\cdot}59\Phi - 14\,992$
	$r^2 = 0{\cdot}274$, $p < 0{\cdot}01$	$r^2 = 0{\cdot}5195$, $p < 0{\cdot}01$
0·25–0·50	$R_f = 1{\cdot}0719\Phi - 36{\cdot}752$	$Y_{s,f} = 202{\cdot}71\Phi - 7009$
	$r^2 = 0{\cdot}1326$, $p < 0{\cdot}05$	$r^2 = 0{\cdot}2711$, $p < 0{\cdot}01$
0·50–1·0	$R_f = 0{\cdot}3224\Phi - 11{\cdot}375$	$Y_{s,f} = 120{\cdot}81\Phi - 4095{\cdot}7$
	$r^2 = 0{\cdot}2683$, $p < 0{\cdot}01$	$r^2 = 0{\cdot}0943$, $p < 0{\cdot}01$

DOI: 10.1002/esp

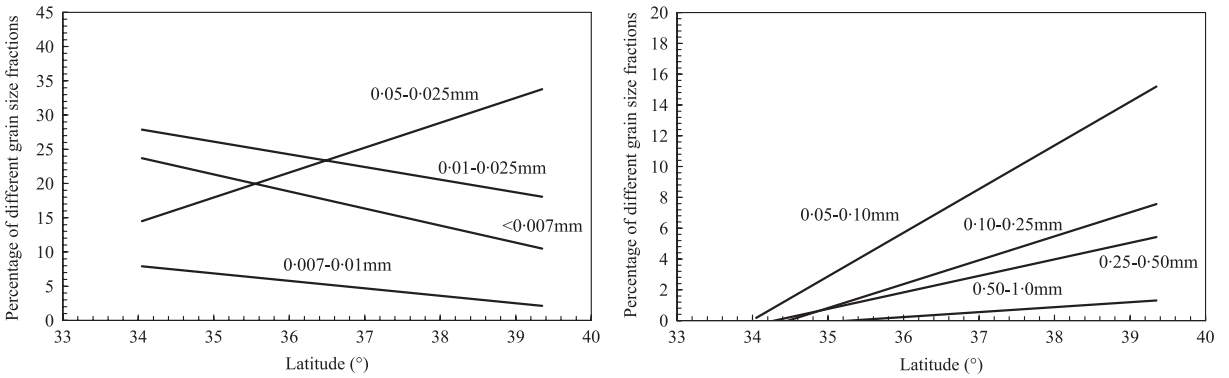

Figure 11. Regression lines for the latitudinal variation of the percentage in suspended sediment for all eight $Y_{s,f}$.

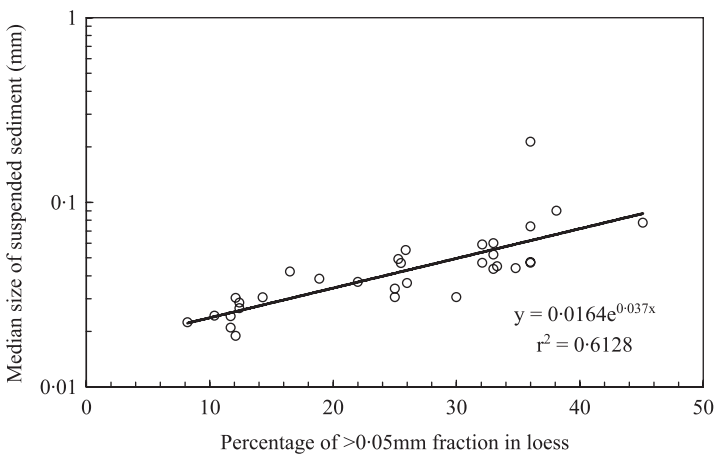

Figure 12. Relationship between median size of suspended sediment and over 0·05 mm percentage in loess in the drainage basin, based on some tributaries of the middle Yellow River.

Table III. Correlation matrix between Y_s and some influencing variables

	$\ln(D_{ss})$	$\ln(P_m)$	$\ln(r_{<0·007})$	$\ln(r_{0·007–0·01})$	$\ln(r_{0·05–0·10})$	$\ln(r_{0·025–0·05})$	$\ln(r_{0·05–0·10})$	$\ln(r_{0·10–0·25})$	$\ln(Y_s)$
$\ln(D_{ss})$	1·00	−0·80	−0·85	−0·77	−0·81	−0·44	0·49	0·63	0·71
$\ln(P_m)$	−0·80	1·00	0·74	0·69	0·75	0·26	−0·50	−0·54	−0·83
$\ln(r_{<0·007})$	−0·85	0·74	1·00	0·79	0·81	0·45	−0·36	−0·51	−0·70
$\ln(r_{0·007–0·01})$	−0·77	0·69	0·79	1·00	0·90	0·47	−0·65	−0·71	−0·68
$\ln(r_{0·05–0·10})$	−0·81	0·75	0·81	0·90	1·00	0·55	−0·64	−0·76	−0·67
$\ln(r_{0·025–0·05})$	−0·44	0·26	0·45	0·47	0·55	1·00	0·13	−0·60	−0·02
$\ln(r_{0·05–0·10})$	0·49	−0·50	−0·36	−0·65	−0·64	0·13	1·00	0·55	0·61
$\ln(r_{0·10–0·25)}$	0·63	−0·54	−0·51	−0·71	−0·76	−0·60	0·55	1·00	0·38
$\ln(Y_s)$	0·71	−0·83	−0·70	−0·68	−0·67	−0·02	0·61	0·38	1·00

including P_m, D_{ss} and percentages of six grain size fractions in suspended sediment (namely <0·007 mm ($r_{<0·007}$), 0·007–0·01 mm ($r_{0·007–0·01}$), 0·01–0·025 mm ($r_{0·01–0·025}$), 0·025–0·05 mm ($r_{0·025–0·05}$), 0·05–0·10 mm ($r_{0·05–0·10}$) and 0·10–0·25 mm ($r_{0·10–0·25}$)) is shown in Table III. The grain size fractions coarser than 0·25 mm are not included because for many rivers these fractions do not appear in suspended sediment. For some of the rivers the data of one or more variables are missing and in total we had 33 rivers where data for all the above variables are available.

Based on data from these rivers, forward stepwise multiple regression analyses were performed, with the critical F-value being set as 4·0. As a result, the following equation has been established:

DOI: 10.1002/esp

$$Y_s = 1{\cdot}048 \times 10^{13} P_m^{-3{\cdot}288} r_{0{\cdot}05-0{\cdot}10}^{0{\cdot}559} r_{0{\cdot}10-0{\cdot}25}^{-0{\cdot}283} r_{<0{\cdot}007}^{-0{\cdot}698} \quad (1)$$

where number of samples $N = 33$, multiple correlation coefficient $R = 0{\cdot}898$, the result of the F-test is $F = 29{\cdot}287$, with the probability of significance $p = 1{\cdot}22 \times 10^{-9}$, and the standard error of estimate is SE = 0·462(log units). The order of the influencing variables in the equation is the same as the order in which they entered the equation during the calculation of stepwise regression analysis. It is notable that D_{ss} failed to enter the equation because there is close correlation between P_m and D_{ss} ($r = 0{\cdot}80$), and the effect of D_{ss} can be reflected by P_m. Of the six indices for sediment grain size, three enter the equation. The directions in which the three indices affect sediment yield are different. Different grain size fractions in surface material play may different roles in runoff generation and erosion process. The fraction finer than 0·007 mm reflects the cohesive clay content in the surface material. The higher $r_{<0{\cdot}007}$ is, the lower the erodibility of the surface material. Thus, with the increase in $r_{<0{\cdot}007}$, Y_s decreases as the equation shows. The effect of relatively coarse fractions in surface material is twofold. The higher the relatively coarse fractions in surface material are, the less cohesive the surface material is, and then the higher its erodibility is. On the other hand, the higher the relatively coarse fractions in the surface material are, the higher its permeability is, and then the less runoff will be generated with given rainfall, which may result in a lower runoff erosivity. For the fraction between 0·05 and 0·10 mm, the first effect may be dominant, and then with the increase in $r_{0{\cdot}05-0{\cdot}10}$ Y_s increases as the equation shows. However, for the fraction between 0·10 and 0·25 mm, the second effect may be dominant, and then with the increase in $r_{0{\cdot}10-0{\cdot}25}$ Y_s decreases as the equation shows.

Since D_{ss} failed to enter the above equation, we established the multiple regression equation between Y_s and P_m and D_{ss} to show how Y_s is influenced by precipitation and sand–dust storms. The equation is as follows:

$$Y_s = 2{\cdot}759 \times 10^{14} P_m^{-3{\cdot}940} D_{ss}^{0{\cdot}112} \quad (2)$$

where $N = 33$, $R = 0{\cdot}835$, the result of the F-test is $F = 34{\cdot}539$, with the probability of significance $p = 2{\cdot}92 \times 10^{-6}$, and the standard error of estimate is SE = 0·560(log units).

As the range of the absolute values of the two influencing variables differs from each other, the regression coefficients of the independent variables do not reflect their contribution to the dependent variable. Therefore, the data have been standardized to the range of (0, 1), and then the multiple regression equation is re-established as follows:

$$Y_s = P_m^{-0{\cdot}725} D_{ss}^{0{\cdot}133} \quad (3)$$

By comparing the regression coefficients (i.e. the components) of P_m and D_{ss}, they can be ranked in terms of their contribution to the variation in Y_s. The contribution of the two influencing variables may be thought of as being in proportion with the absolute values of their components in the equation. Thus, the contributions of P_m and D_{ss} were calculated as 84·5 and 15·5%, respectively. This indicates that precipitation plays much more important role in determining sediment yield in the Loess Plateau region.

Table I and Figure 7 show the different ways in which annual precipitation and annual sand–dust storms influence specific sediment yield of different grain size fractions. To reveal this difference further, we established the regression equation between the fractional specific sediment yield ($Y_{s,f}$) and two influencing variables (P_m and D_{ss}) for each grain size fraction separately, and the results are shown in Table IV. To assess the contribution of P_m and D_{ss} to $Y_{s,f}$, equations based on the data standardized to the range of (0, 1) are also established. From these equations, the contributions of P_m and D_{ss} to $Y_{s,f}$ were calculated. The results are also shown in Table III.

Table IV shows that with the increase in grain size, the multiple correlation coefficient increases. For all equations the contribution of P_m to $Y_{s,f}$ is larger than that of D_{ss}, indicating that precipitation has greater influence on sediment yield than sand–dust storms have. The contribution of P_m to $Y_{s,f}$ decreases with the increased grain size, and the contribution of D_{ss} to $Y_{s,f}$ increases with the increased grain size (Figure 13), indicating that the fractional sediment yield of coarser grain sizes depends more on sand–dust storms than on precipitation. These results can be used for drainage basin management and sediment control for the Yellow River. Apart from controlling erosion and sediment yield by water, controlling erosion and sediment yield by wind is also important, especially for controlling the yield of relative coarse sediment, which causes more deposition in the lower Yellow River than fine sediment (Chien *et al.*, 1980).

Conclusions

Based on data from 35 stations on the tributaries of the Yellow River, annual specific sediment yield (Y_s) in eight grain size fractions has been related to basin-averaged annual sand–dust storm days (D_{ss}) and annual precipitation (P_m), to reveal the influence of eolian and fluvial processes on specific sediment yield in different grain size fractions.

DOI: 10.1002/esp

Table IV. Regression equation between the fractional specific sediment yield ($Y_{s,f}$) and two influencing variables (P_m and D_{ss}) for each grain size fraction

Grain size fractions (mm)	Regression equation	Regression equation after data standardization	R	Contribution of P_m to $Y_{s,f}$	Contribution of D_{ss} to $Y_{s,f}$
<0·007	$Y_{s,f} = 7{\cdot}75 \times 10^{12} P_m^{-3{\cdot}62} D_{ss}^{-0{\cdot}12}$	$Y_{s,f} = P_m^{-0{\cdot}85} D_{ss}^{-0{\cdot}19}$	0·71	82·1	17·9
0·007–0·01	$Y_{s,f} = 3{\cdot}11 \times 10^{11} P_m^{-3{\cdot}60} D_{ss}^{-0{\cdot}17}$	$Y_{s,f} = P_m^{-0{\cdot}81} D_{ss}^{-0{\cdot}27}$	0·62	74·8	25·2
0·01–0·025	$Y_{s,f} = 3{\cdot}03 \times 10^{11} P_m^{-3{\cdot}10} D_{ss}^{-0{\cdot}15}$	$Y_{s,f} = P_m^{-0{\cdot}75} D_{ss}^{-0{\cdot}24}$	0·59	75·7	24·3
0·025–0·05	$Y_{s,f} = 1{\cdot}87 \times 10^{15} P_m^{-4{\cdot}46} D_{ss}^{-0{\cdot}086}$	$Y_{s,f} = P_m^{-0{\cdot}77} D_{ss}^{-0{\cdot}096}$	0·70	89·0	11·0
0·05–0·1	$Y_{s,f} = 3{\cdot}49 \times 10^{12} P_m^{-4{\cdot}99} D_{ss}^{0{\cdot}26}$	$Y_{s,f} = P_m^{-0{\cdot}61} D_{ss}^{0{\cdot}20}$	0·78	75·0	25·0
0·1–0·25	$Y_{s,f} = 2{\cdot}36 \times 10^{14} P_m^{-4{\cdot}49} D_{ss}^{0{\cdot}59}$	$Y_{s,f} = P_m^{-0{\cdot}49} D_{ss}^{0{\cdot}41}$	0·86	54·4	45·6
0·25–0·50	$Y_{s,f} = 5{\cdot}53 \times 10^{13} P_m^{-4{\cdot}44} D_{ss}^{0{\cdot}58}$	$Y_{s,f} = P_m^{-0{\cdot}46} D_{ss}^{0{\cdot}39}$	0·80	54·2	45·8
0·50–1·0	$Y_{s,f} = 1{\cdot}27 \times 10^{21} P_m^{-7{\cdot}20} D_{ss}^{0{\cdot}48}$	$Y_{s,f} = P_m^{-0{\cdot}55} D_{ss}^{0{\cdot}31}$	0·84	63·9	36·1

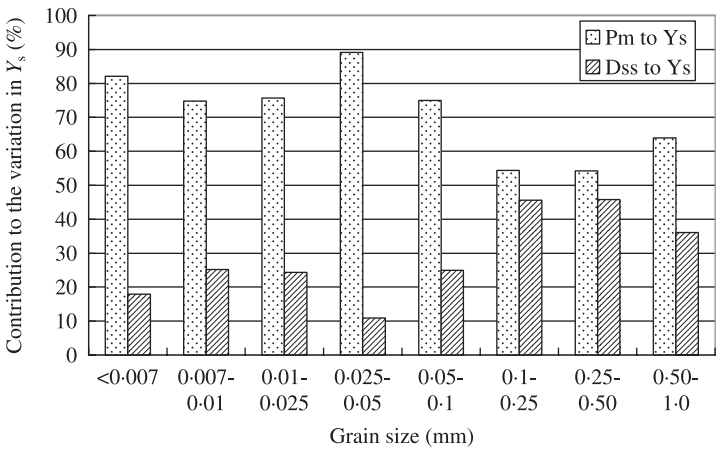

Figure 13. Histogram of the contribution of P_m and D_{ss} to $Y_{s,f}$.

The results show that Y_s in fine grain size fractions has the highest values in the areas dominated by the coupled wind–water process. From these areas to those dominated by eolian process or to those dominated by the fluvial process, Y_s tends to decrease. For relatively coarse grain size fractions, Y_s has monotonic variation, i.e. with increase in D_{ss} or decrease in P_m, Y_s increases. This indicates that the sediment producing behavior for fine sediments is different from that for relatively coarse sediments.

The results all show that Y_s for relatively coarse sediments depends on eolian process more than on fluvial process, and the coarser the sediment fractions, the stronger the dependence of Y_s on the eolian process. The Y_s–D_{ss} and Y_s–P_m curves for fine grain size fractions show some peaks and the fitted straight lines for Y_s–D_{ss} and Y_s–P_m relationships for relatively coarse grain size fractions show some breaks. Almost all these break points may be regarded as thresholds. These thresholds are all located in the areas dominated by the coupled wind–water process, indicating that these areas are sensitive for erosion and sediment producing, to which more attention should be given for the purpose of erosion and sediment control.

A number of regression equations were established, based which the effect of rainfall, sand–dust storms and surface material grain size on specific sediment yield can be assessed.

Acknowledgements

The financial support from the Third-Phase Knowledge Innovation Program of the Institute of Geographical Sciences and Natural Resources Research, Chinese Academy of Sciences and the National Natural Science Foundation of China (40271019) is gratefully acknowledged. Thanks are also expressed to the Yellow River Water Conservancy Commission, for permission to access hydrometric data, and to two anonymous reviewers, whose comments and suggestions have been invaluable for improving the manuscript.

DOI: 10.1002/esp

References

American Society of Civil Engineers (ASCE) Task Committee on Preparation of Sedimentation Manual. 1975. *Sedimentation Engineering*, ASCE M and R No. 54, Vanoni VA (ed.).

Asselman NEM. 1999. Suspended sediment dynamics in a large drainage basin: the River Rhine. *Hydrological Processes* **13**(10): 1437–1450.

Chien N, Wan ZH. 1998. *Mechanics of Sediment Transport*. ASCE Press: Reston, VA; 523–619.

Chien N, Wang KX, Yan LD, Fu RS. 1980. The source of coarse sediment in the middle reaches of the Yellow River and its effect on the siltation of the lower Yellow River. In *Proceedings of the First International Symposium on River Sedimentation held in Beijing*. Chinese Society of Hydraulic Engineering; 53–62.

Compilation Commission of Bulletin of River Sedimentation in China. 2003. *Bulletin of River Sedimentation in China* (2002). Chinese Ministry of Water Resources.

Grimshaw DL, Lewin J. 1980. Source identification for suspended sediments. *Journal of Hydrology* **47**: 51–162.

Langbein LB, Schumm SA. 1958. Yield of sediment in relation to mean annual precipitation. *Transactions American Geophysical Union* **39**: 1076–1084.

Liu DS. 1964. Loess in the Middle Yellow River Basin. Science: Beijing (in Chinese).

Peart MR, Walling DE. 1982. *Particle Size Characteristics of Fluvial Suspended Sediment*, International Association of Hydrological Sciences Publication **137**; 397–407.

Reid I, Frostick LE. 1994. Fluvial sediment transport and deposition. In *Sediment Transport and Depositional Processes*, Pye IC (ed.). Blackwell: Oxford; 9–155.

Tang KL (ed.). 1990. Regional Characteristics of Soil Erosion and its Control on the Loess Plateau. Chinese Press for Science and Technology: Beijing; 118–152 (in Chinese).

Walling DE, Moorehead PW. 1987. Spatial and temporal variation of the particle-size characteristics of fluvial sediment. Geografiska Annaler **69A**(1): 47–59.

Walling DE, Moorehead PW. 1989. The particle size characteristics of fluvial sediment: an overview. *Hydrobiologia* **176/177**: 125–149.

Walling DE, Webb BW. 1992. Water quality: I. Physical characteristics. In *The River Handbook*, Calow P, Petts G (eds). Blackwell: London; 48–72.

Xu JH, Niu YG. 2000. A Study of Runoff and Sediment Yield as Influenced by Soil and Water Conservation and Hydraulic Engineering Works in the Middle Yellow River Basin. Publishing House for Yellow River's Water Conservancy: Zhengzhou (in Chinese).

Xu JX. 1997. The optimal grainsize composition of suspended sediment of hyperconcentrated flows in the middle Yellow River. *International Journal of Sediment Research* **12**(3): 170–176.

Xu JX. 1998. A study of physico-geographical factors for formation of hyperconcentrated flows in the Loess Plateau of China. *Geomorphology* **24**: 245–255.

Xu JX. 2002a. Complex behaviours of natural sediment-carrying streamflows and the geomorphological implications. *Earth Surface Processes and Landforms* **27**(7): 749–758.

Xu JX. 2002b. Implication of relationships among suspended sediment size, water discharge and suspended sediment concentration: the Yellow River basin, China. *Catena* **49**(4): 289–307.

Xu JX. 2005a. Influences of coupled wind–water processes on suspended sediment grain size: an example from tributaries of the Yellow River. *Hydrological Science Journal* **50**(5): 881–896.

Xu JX. 2005b. Physico-geographical factors for the formation of sand–dust storms in the Loess Plateau region. *Deserts in China* **25**(4): 552–556 (in Chinese).

Xu JX, Cheng DS. 2002. Relation between the erosion and sedimentation zones in the Yellow River, China. *Geomorphology* **48**(4): 365–382.

Xu JX, Yan YX. 2005. Scale effect on specific sediment yield in the Yellow River basin and some geomorphological implications. *Journal of Hydrology* **307**(1–4): 219–232.

Xu JX, Yang JS, Yan YX. 2006. Erosion and sediment yield as influenced by coupled eolian and fluvial processes: the Yellow River, China. *Geomorphology* **73**(1): 1–15.

Zhao WL (ed.). 1996. Sedimentation of the Yellow River. Yellow River Water Conservancy Press: Zhengzhou (in Chinese).

Zhu BH. 1982. A Dictionary of Meteorology. Shanghai Publishing House for Dictionaries: Shanghai; 38 (in Chinese).